

# Measurements of the angle $\alpha$ ( $\phi_2$ ) at B factories

G. Vasseur

CEA, Irfu, SPP, Centre de Saclay, F-91191 Gif sur Yvette, France

The measurements of the angle  $\alpha$  ( $\phi_2$ ) of the unitarity triangle at the B factories are reviewed. The value of  $\alpha$  determined by combining the results obtained in the  $B \rightarrow \pi\pi$ ,  $B \rightarrow \rho\pi$ , and  $B \rightarrow \rho\rho$  modes by both the BABAR and Belle experiments is  $(87.5_{-5.3}^{+6.2})^\circ$ .

## 1. Introduction

### 1.1. The angle $\alpha$

In the Standard Model (SM),  $CP$  violation in the quark sector is explained through the complex Cabibbo-Kobayashi-Maskawa (CKM) quark-mixing matrix [1]. One relation due to the unitarity of the CKM matrix,  $V_{ud}V_{ub}^* + V_{cd}V_{cb}^* + V_{td}V_{tb}^* = 0$ , is represented graphically in the complex plane as the unitarity triangle, shown in Figure 1.

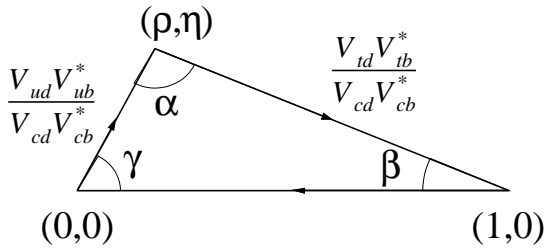


Figure 1: The unitarity triangle.

The goal of the BABAR and Belle experiments is to test the SM explanation of  $CP$  violation in overconstraining the unitarity triangle, by measuring its sides and its three angles  $\alpha$ ,  $\beta$ , and  $\gamma$  (also called  $\phi_2$ ,  $\phi_1$ , and  $\phi_3$  respectively). The angle  $\alpha = \arg(-\frac{V_{td}V_{tb}^*}{V_{ud}V_{ub}^*})$  brings into play the two elements of the CKM matrix which are non real at lowest order:  $V_{ub}$ , involved in decays proceeding via a  $b$  to  $u$  transition, whose phase is  $-\gamma$ , and  $V_{td}$ , involved in  $B^0\bar{B}^0$  mixing, whose phase is  $-\beta$ . So  $\alpha = \pi - \beta - \gamma$  can be measured from  $CP$  violating asymmetries in the interference between mixing and decay in charmless decays of the neutral  $B$  mesons, such as  $B^0 \rightarrow \pi^+\pi^-$ ,  $B^0 \rightarrow \rho^+\rho^-$ ,  $B^0 \rightarrow \pi^+\pi^-\pi^0$ , and  $B^0 \rightarrow a_1^\pm\pi^\mp$ .

### 1.2. Time-dependent $CP$ asymmetry

A  $B^0$  meson can decay into a  $CP$  eigenstate  $f$  either directly or after having oscillated to a  $\bar{B}^0$  meson which then decays to  $f$ . The amplitudes associated to the two processes are respectively  $A_f$  and  $\frac{q}{p}\bar{A}_f$  where  $\frac{q}{p} \sim e^{-2i\beta}$  accounts for  $B^0\bar{B}^0$  mixing. The resulting  $CP$

violation asymmetry as a function of the proper time difference  $\Delta t$  can be expressed as:

$$a_f(\Delta t) = \frac{\Gamma_{\bar{B}^0 \rightarrow f}(\Delta t) - \Gamma_{B^0 \rightarrow f}(\Delta t)}{\Gamma_{\bar{B}^0 \rightarrow f}(\Delta t) + \Gamma_{B^0 \rightarrow f}(\Delta t)} = S \sin(\Delta m \Delta t) - C \cos(\Delta m \Delta t) \quad (1)$$

where  $\Delta m$  is the mass difference between the two neutral  $B$  mass eigenstates. The coefficients  $C = \frac{1-|\lambda_f|^2}{1+|\lambda_f|^2}$  and  $S = \frac{2\Im(\lambda_f)}{1+|\lambda_f|^2}$  are functions of the ratio of the amplitudes with and without mixing  $\lambda_f = \frac{q}{p}\frac{\bar{A}_f}{A_f}$ .  $C$  (or  $\mathcal{A} = -C$ ) measures direct  $CP$  violation while  $S$  measures  $CP$  violation in the interference between decay and mixing.

In the simple case of a charmless  $B^0$  decay involving only the  $b$  to  $u$  tree diagram amplitude, with weak phase  $\gamma$ , we have  $\lambda_f = e^{-2i\beta}e^{-2i\gamma} = e^{2i\alpha}$ , resulting in  $C = 0$  and  $S = \sin 2\alpha$ . A time-dependent analysis of the  $CP$  asymmetry in this mode would give a direct measurement of  $\alpha$ . However other diagrams are involved in charmless decays and in particular the one loop gluonic penguin diagrams. As the dominant gluonic penguin diagram does not carry the same weak phase as the tree diagram, the extraction of  $\alpha$  becomes more complex.  $C$  is no longer equal to 0 and  $S = \sqrt{1-C^2} \sin 2\alpha_{\text{eff}}$  does not any more measure  $\alpha$  but an effective value  $\alpha_{\text{eff}}$ .

### 1.3. The isospin analysis

The isospin analysis [2], based on  $SU(2)$  symmetry, allows the extraction of the true value of  $\alpha$ . It can be applied both to the  $B \rightarrow \pi\pi$  and  $B \rightarrow \rho\rho$  modes and uses all the  $B$  decay modes to  $hh$  ( $h = \pi$  or  $\rho$ ) to determine the difference  $\alpha - \alpha_{\text{eff}}$ . Tree and penguin contributions to  $B \rightarrow hh$  decays are summarized in Table I. Since the tree amplitude in the  $B^0 \rightarrow h^0h^0$  decays is color suppressed, the branching ratio of these modes is expected to be small. Also the isospin conservation rules exclude gluonic penguin transitions for  $h^+h^0$  final states.

The  $SU(2)$  isospin symmetry relates the amplitudes of all the  $B \rightarrow hh$  modes:  $A^{+-} = A(B^0 \rightarrow h^+h^-)$ ,  $A^{+0} = A(B^+ \rightarrow h^+h^0)$ ,  $A^{00} = A(B^0 \rightarrow h^0h^0)$ ,  $\tilde{A}^{+-} = A(\bar{B}^0 \rightarrow h^+h^-)$ ,  $\tilde{A}^{-0} = A(B^- \rightarrow h^-h^0)$ ,

Table I Diagrams contributing to  $B \rightarrow hh$  decays.

Mode	Tree	Gluonic penguin
$h^+h^-$	Color-allowed	Present
$h^0h^0$	Color-suppressed	Present
$h^+h^0$	Color-allowed	Forbidden

and  $\tilde{A}^{00} = A(\bar{B}^0 \rightarrow h^0h^0)$ . Neglecting electroweak penguins and other  $SU(2)$ -breaking effects, we obtain the isospin relations:

$$\frac{A^{+-}}{\sqrt{2}} + A^{00} = A^{+0} = \tilde{A}^{-0} = \frac{\tilde{A}^{+-}}{\sqrt{2}} + \tilde{A}^{00} \quad (2)$$

where we used the fact that the amplitude of the pure tree  $B^+ \rightarrow h^+h^0$  mode is equal to the one of its charge conjugate process.

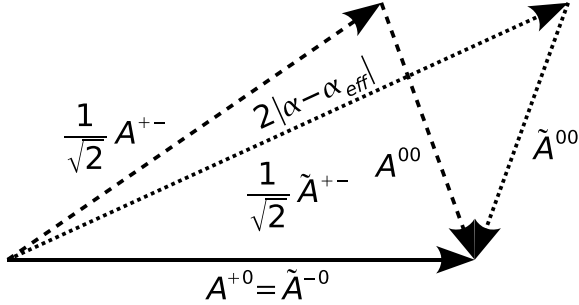


Figure 2: Graphical representation of the isospin relations.

These relations are represented graphically as two triangles with a common base, shown in Figure 2. Measuring the lengths of the sides of the two triangles, related to the branching ratios of the various modes, constrains  $\alpha - \alpha_{\text{eff}}$ . As both triangles have two possible orientations, up and down, the isospin method has a four-fold ambiguity, which comes in addition to the two-fold ambiguity related to the fact that only the sine of  $2\alpha_{\text{eff}}$  is measured in the time-dependent analysis of  $B^0 \rightarrow h^+h^-$ .

#### 1.4. Analyses overview

The *BABAR* and Belle detectors at the PEP-II and KEK-B colliders respectively are described in details elsewhere [3].

At the  $\Upsilon(4S)$  resonance,  $B\bar{B}$  pairs are produced in a coherent state. The  $CP$  asymmetry is measured as a function of the difference between the decay times of the two  $B$  mesons  $\Delta t$ , which in an energy asymmetric machine is obtained from the measured distance along the beam axis between the two vertices  $\Delta z$  according to  $\Delta t = \Delta z/\beta\gamma c$ . Here  $c$  is the speed of light and

$\beta\gamma$ , equal to 0.56 in *BABAR* and 0.425 in Belle, is the Lorentz boost of the  $\Upsilon(4S)$ .

One of the  $B$  mesons is fully reconstructed into the  $B$  decay of interest ( $\pi\pi$ ,  $\rho\pi$ ,  $\rho\rho$ , or  $a_1\pi$ ), while the other  $B$  meson is used to tag its flavor at production time. Tagging combines different techniques including the use of semileptonic decays and secondary kaons.

To select the signal, hadron identification is used to separate pions from kaons. The beam energy constrained  $B$ -meson mass  $m_B = \sqrt{E_{\text{beam}}^2 - p_B^2}$  and the energy difference  $\Delta E = E_B - E_{\text{beam}}$  are powerful kinematic discriminating variables, peaking respectively for the signal at the  $B$ -meson mass and zero.  $E_{\text{beam}}$  is the beam energy.  $E_B$  and  $p_B$  are the energy and momentum of the reconstructed candidate, all evaluated in the  $\Upsilon(4S)$  rest frame.

The largest background consists of  $q\bar{q}$  ( $q = u, d, s, c$ ) continuum events. The  $B\bar{B}$  events look spherical while the continuum events are jet-like, so event shape variables are also used for separation.

The following results are based on multi-variable maximum likelihood analyses.

## 2. Results from $B \rightarrow \pi\pi$ decays

The time-dependent  $CP$  asymmetry of the  $B^0 \rightarrow \pi^+\pi^-$  decays has been studied by Belle using  $535 \times 10^6$   $B\bar{B}$  pairs [4] and by *BABAR* using  $383 \times 10^6$   $B\bar{B}$  pairs [5]. Fits that include respectively  $1464 \pm 65$  signal events for Belle and  $1139 \pm 49$  for *BABAR* give measurements of  $S_{\pi^+\pi^-}$  and  $C_{\pi^+\pi^-}$ , summarized in Table II. Both experiments have observed  $CP$  violation in the interference between decay and mixing in the  $B^0 \rightarrow \pi^+\pi^-$  decays as the  $S_{\pi^+\pi^-}$  parameter is found different from 0 with a significance of  $5.3\sigma$  for Belle and  $5.1\sigma$  for *BABAR* with a perfect agreement between the two experiments. In addition Belle sees a  $5.5\sigma$  effect also for the direct  $CP$  violation parameter  $C_{\pi^+\pi^-}$ , which is different from the *BABAR* result, at the level of  $2.1\sigma$ , but not inconsistent with it.

All the  $B \rightarrow \pi\pi$  modes, which are needed to perform the isospin analysis, have been measured by *BABAR* and Belle. The measurements from *BABAR* are based on  $227 \times 10^6$   $B\bar{B}$  pairs for  $B^0 \rightarrow \pi^+\pi^-$  [6] and on  $383 \times 10^6$   $B\bar{B}$  pairs for  $B^+ \rightarrow \pi^+\pi^0$  and  $B^0 \rightarrow \pi^0\pi^0$  [7], while those from Belle use  $449 \times 10^6$   $B\bar{B}$  pairs for  $B^0 \rightarrow \pi^+\pi^-$  and  $B^+ \rightarrow \pi^+\pi^0$  [8] and  $535 \times 10^6$   $B\bar{B}$  pairs for  $B^0 \rightarrow \pi^0\pi^0$  [9] and for the  $CP$  asymmetry in  $B^+ \rightarrow \pi^+\pi^0$  [10]. The results and the world averages [11] for the branching ratios over the charge conjugate processes, as well as the time-integrated charge asymmetries  $\mathcal{A}$  are given in Table II. The branching ratio of  $B^0 \rightarrow \pi^0\pi^0$ , whose tree diagram is color suppressed, is relatively large, about one fourth of that of  $B^0 \rightarrow \pi^+\pi^-$ , thus indicating a large penguin contamination in  $B \rightarrow \pi\pi$ . The charge asymmetry in  $B^+ \rightarrow \pi^+\pi^0$  is compatible with 0 as expected.

Table II Measurements of  $CP$  parameters and branching fractions in the  $B \rightarrow \pi\pi$  modes.

	BABAR	Belle	World average
$S_{\pi^+\pi^-}$	$-0.60 \pm 0.11 \pm 0.03$	$-0.61 \pm 0.10 \pm 0.04$	$-0.61 \pm 0.08$
$C_{\pi^+\pi^-}$	$-0.21 \pm 0.09 \pm 0.02$	$-0.55 \pm 0.08 \pm 0.05$	$-0.38 \pm 0.07$
$A_{\pi^+\pi^0}$	$0.03 \pm 0.08 \pm 0.01$	$0.07 \pm 0.06 \pm 0.01$	$0.06 \pm 0.05$
$A_{\pi^0\pi^0}$	$0.5 \pm 0.4 \pm 0.1$	$0.4 \pm 0.7 \pm 0.1$	$0.5 \pm 0.3$
$\mathcal{B}(B^0 \rightarrow \pi^+\pi^-)$	$(5.5 \pm 0.4 \pm 0.3)10^{-6}$	$(5.1 \pm 0.2 \pm 0.2)10^{-6}$	$(5.2 \pm 0.2)10^{-6}$
$\mathcal{B}(B^+ \rightarrow \pi^+\pi^0)$	$(5.0 \pm 0.5 \pm 0.3)10^{-6}$	$(6.5 \pm 0.4 \pm 0.5)10^{-6}$	$(5.6 \pm 0.4)10^{-6}$
$\mathcal{B}(B^0 \rightarrow \pi^0\pi^0)$	$(1.5 \pm 0.3 \pm 0.1)10^{-6}$	$(1.1 \pm 0.3 \pm 0.1)10^{-6}$	$(1.3 \pm 0.2)10^{-6}$

Using the six observables (the branching fraction of the three  $B \rightarrow \pi\pi$  modes,  $S_{\pi^+\pi^-}$ ,  $C_{\pi^+\pi^-}$ , and  $A_{\pi^0\pi^0}$ ) an isospin analysis is performed to determine the six unknown parameters and in particular  $\alpha$ . The constraint on  $\alpha$  is illustrated by the confidence level plot from the CKMfitter group [12] in Figure 3. The already mentioned 8-fold ambiguity in the determination of  $\alpha$  corresponds to the eight peaks which can be seen on this plot. Choosing the peak consistent with the other CKM measurements, the combined determination of  $\alpha$  from the  $B \rightarrow \pi\pi$  modes is  $(92^{+11}_{-10})^\circ$ . The range of values between  $14^\circ$  and  $76^\circ$  is excluded at 95% C.L.

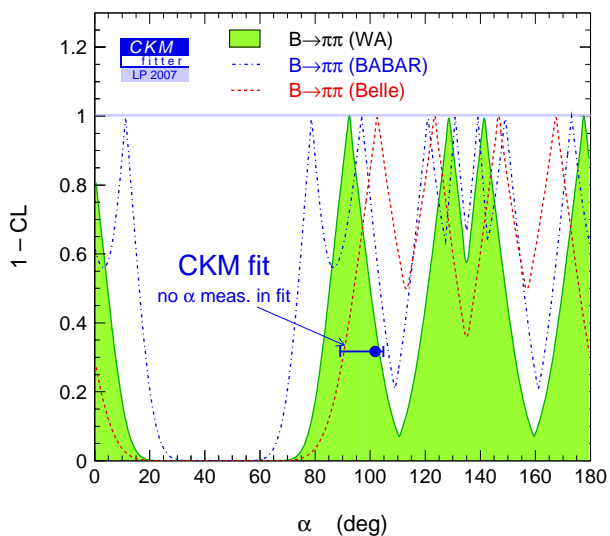


Figure 3: Constraint on  $\alpha$  from the isospin analysis in the  $B \rightarrow \pi\pi$  modes. The dot-dashed (dashed) curve uses BABAR (Belle) measurements only, while the hatched region gives the combined constraint.

### 3. Results from $B \rightarrow \rho\rho$ decays

$B \rightarrow \rho\rho$  analyses are experimentally more challenging than the  $B \rightarrow \pi\pi$  analyses as the final states consist of four pions, including two  $\pi^0$  for the  $\rho^+\rho^-$  mode. The wide  $\rho$  resonances also result in more background. Finally these vector-vector modes are not  $CP$  eigenstates.

But as the  $B^0 \rightarrow \rho^+\rho^-$  mode is almost 100% longitudinally polarized, an analysis of the sole longitudinal  $CP$ -even component is adequate. Besides the branching ratio for  $B^0 \rightarrow \rho^+\rho^-$  is about five times larger than for  $B^0 \rightarrow \pi^+\pi^-$ , and the ratio of penguin over tree amplitude is smaller. Thus this mode turns out to be better for constraining  $\alpha$ .

A similar analysis to that for  $B^0 \rightarrow \pi^+\pi^-$  is performed for the  $B^0 \rightarrow \rho^+\rho^-$  mode, with the reconstructed masses of the two  $\rho$  mesons as well as their helicity angles as additional observables, and the fraction  $f_L$  of longitudinal polarization as an additional parameter. The decay rate as a function of  $f_L$  and the helicity angles  $\theta_{1,2}$  is:  $\frac{d\Gamma}{d\theta_1 d\theta_2} \propto \frac{1-f_L}{4} \sin^2 \theta_1 \sin^2 \theta_2 + f_L \cos^2 \theta_1 \cos^2 \theta_2$ .

Using respectively  $576 \pm 53$  signal events from a sample of  $535 \times 10^6 B\bar{B}$  pairs [13] and  $729 \pm 60$  signal events from a sample of  $383 \times 10^6 B\bar{B}$  pairs [14], the Belle and BABAR experiments have measured the  $CP$  parameters  $S_{\rho^+\rho^-}$  and  $C_{\rho^+\rho^-}$ , given in Table III.

The other ingredients for the isospin analysis, the branching fractions, fractions of longitudinal polarization and remaining  $CP$  parameters, have been measured by Belle using  $275 \times 10^6 B\bar{B}$  pairs for  $B^0 \rightarrow \rho^+\rho^-$  [15],  $85 \times 10^6 B\bar{B}$  pairs for  $B^+ \rightarrow \rho^+\rho^0$  [16], and  $657 \times 10^6 B\bar{B}$  pairs for  $B^0 \rightarrow \rho^0\rho^0$  [17], and by BABAR using  $383 \times 10^6 B\bar{B}$  pairs for  $B^0 \rightarrow \rho^+\rho^-$  [14],  $232 \times 10^6 B\bar{B}$  pairs for  $B^+ \rightarrow \rho^+\rho^0$  [18], and  $427 \times 10^6 B\bar{B}$  pairs for  $B^0 \rightarrow \rho^0\rho^0$  [19].

The small value of the  $B^0 \rightarrow \rho^0\rho^0$  branching ratio compared to the one of the other channels shows that the penguin contributions are small in the  $B \rightarrow \rho\rho$  modes. The two experiments obtain somewhat different results for the  $B^0 \rightarrow \rho^0\rho^0$  mode, though not inconsistent. While Belle does not see any significant signal, BABAR finds evidence for this decay based on

Table III Measurements of  $CP$  parameters, branching fractions, and fractions of longitudinal polarization in the  $B \rightarrow \rho\rho$  modes.

	BABAR	Belle	World average
$S_{\rho^+\rho^-}$	$-0.17 \pm 0.20 \pm 0.06$	$0.19 \pm 0.30 \pm 0.08$	$-0.05 \pm 0.17$
$C_{\rho^+\rho^-}$	$0.01 \pm 0.15 \pm 0.06$	$-0.16 \pm 0.21 \pm 0.08$	$-0.06 \pm 0.13$
$A_{\rho^+\rho^0}$	$-0.12 \pm 0.13 \pm 0.10$	$0.00 \pm 0.22 \pm 0.03$	$-0.08 \pm 0.13$
$C_{\rho^0\rho^0}$	$0.4 \pm 0.9 \pm 0.2$	-	$0.4 \pm 0.9$
$S_{\rho^0\rho^0}$	$0.5 \pm 0.9 \pm 0.2$	-	$0.5 \pm 0.9$
$\mathcal{B}(B^0 \rightarrow \rho^+\rho^-)$	$(25 \pm 2 \pm 4)10^{-6}$	$(23 \pm 4 \pm 3)10^{-6}$	$(24 \pm 3)10^{-6}$
$\mathcal{B}(B^+ \rightarrow \rho^+\rho^0)$	$(17 \pm 2 \pm 2)10^{-6}$	$(32 \pm 7_{-7}^{+4})10^{-6}$	$(18 \pm 3)10^{-6}$
$\mathcal{B}(B^0 \rightarrow \rho^0\rho^0)$	$(0.8 \pm 0.3 \pm 0.2)10^{-6}$	$(0.4 \pm 0.4 \pm 0.2)10^{-6}$	$(0.7 \pm 0.3)10^{-6}$
$f_L^{\rho^+\rho^-}$	$0.99 \pm 0.02 \pm 0.02$	$0.94 \pm 0.04 \pm 0.03$	$0.98 \pm 0.02$
$f_L^{\rho^+\rho^0}$	$0.90 \pm 0.04 \pm 0.03$	$0.95 \pm 0.11 \pm 0.02$	$0.91 \pm 0.04$
$f_L^{\rho^0\rho^0}$	$0.70 \pm 0.14 \pm 0.05$	-	$0.70 \pm 0.15$

$85 \pm 28$  signal events with a significance of  $3.6 \sigma$  taking into account the systematics. As the decay vertex of the  $\rho^0\rho^0$  final state can be reconstructed in contrast to  $\pi^0\pi^0$ , a time dependant analysis is possible, leading to the measurement of  $C_{\rho^0\rho^0}$  and  $S_{\rho^0\rho^0}$ . BABAR has demonstrated the feasibility of such an analysis and gives a first measurement of these two  $CP$  parameters, though with a large statistical error.

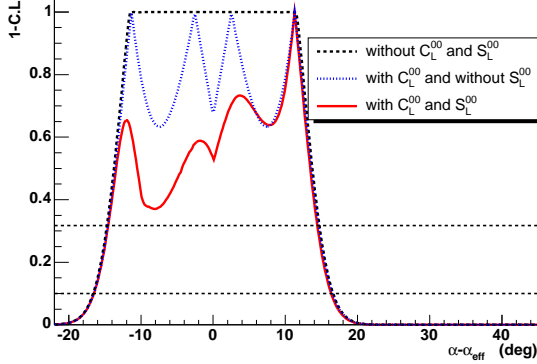


Figure 4: Confidence level on  $\alpha - \alpha_{\text{eff}}$  obtained from the isospin analysis including the measurements of  $C_{\rho^0\rho^0}$  and  $S_{\rho^0\rho^0}$  (solid curve), the measurement of  $C_{\rho^0\rho^0}$  only (dotted curve) and none of them (dashed curve). The horizontal dashed lines correspond to the 68% (top) and 90% (bottom) CL intervals.

Figure 4 shows the impact of measuring these two parameters for the isospin analysis in  $B \rightarrow \rho\rho$  on the confidence level plot for  $\alpha - \alpha_{\text{eff}}$ . Without  $C_{\rho^0\rho^0}$  and  $S_{\rho^0\rho^0}$ , we have only five observables for six unknown parameters and the isospin analysis gives a plateau of degenerated values for  $\alpha - \alpha_{\text{eff}}$ . Adding  $C_{\rho^0\rho^0}$ , we have now as many observables as unknown and find the four ambiguities of the isospin analysis. If we also measure  $S_{\rho^0\rho^0}$ , which gives seven observables for six unknown,

the isospin analysis is able to favor one single solution. With the current statistics, the discrimination between the four solutions is however limited.

Figure 5 shows the outcome of the isospin analysis in the  $B \rightarrow \rho\rho$  modes. Choosing the solution consistent with the other CKM measurements, the combined determination of  $\alpha$  from the  $B \rightarrow \rho\rho$  modes is  $(87_{-11}^{+10})^\circ$ . The range of values between  $20^\circ$  and  $70^\circ$  and the one between  $113^\circ$  and  $156^\circ$  are excluded at 95% C.L.

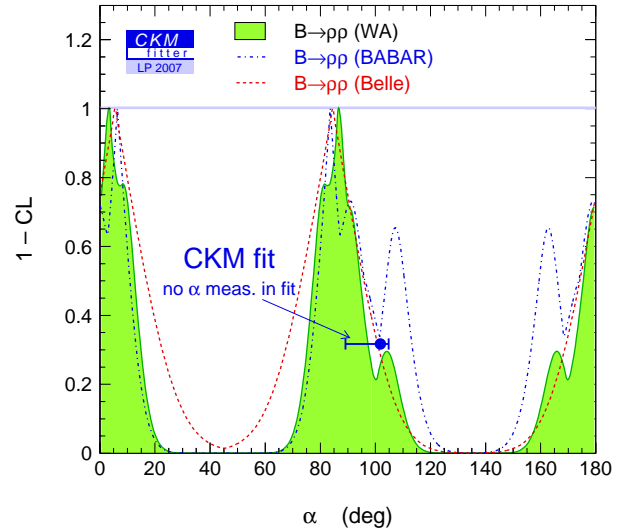


Figure 5: Constraint on  $\alpha$  from the isospin analysis in the  $B \rightarrow \rho\rho$  modes. The dot-dashed (dashed) curve uses BABAR (Belle) measurements only, while the hatched region gives the combined constraint.

An alternative approach to measure  $\alpha$  is to use flavor SU(3) symmetry [20], constraining the penguin contribution in  $B^0 \rightarrow \rho^+\rho^-$  with the longitudinal

Table IV Measurements of the branching fraction, fraction of longitudinal polarization, and  $CP$  parameter in the  $B^+ \rightarrow K^{*0}\rho^+$  modes.

	BABAR	Belle	World average
$\mathcal{B}(B^+ \rightarrow K^{*0}\rho^+)$	$(9.6 \pm 1.7 \pm 1.5)10^{-6}$	$(8.9 \pm 1.7 \pm 1.2)10^{-6}$	$(9.2 \pm 1.5)10^{-6}$
$f_L^{K^{*0}\rho^+}$	$0.52 \pm 0.10 \pm 0.04$	$0.43 \pm 0.11_{-0.002}^{+0.05}$	$0.48 \pm 0.08$
$\mathcal{A}_{K^{*0}\rho^+}$	$-0.01 \pm 0.16 \pm 0.02$	-	$-0.01 \pm 0.16$

part of the SU(3) partner mode: the pure penguin  $B^+ \rightarrow K^{*0}\rho^+$  channel. The latter mode has been measured by Belle using  $275 \times 10^6 B\bar{B}$  pairs [21] and BABAR using  $232 \times 10^6 B\bar{B}$  pairs [22]. This method has three unknowns: the ratio of penguin over tree amplitudes, the relative phase between penguin and tree amplitudes and  $\alpha$ . Taking SU(3) breaking effect into account, it gives a good constraint on  $\alpha$  [14]:  $83 < \alpha < 106^\circ$  at 68 % C.L., illustrated in Figure 6.

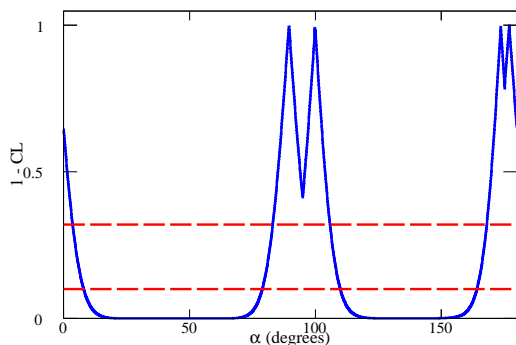


Figure 6: Confidence level on  $\alpha$  from the SU(3) analysis of the  $B^0 \rightarrow \rho^+\rho^-$  and  $B^+ \rightarrow K^{*0}\rho^+$  modes. The horizontal dashed lines correspond to the 68% (top) and 90% (bottom) CL intervals.

#### 4. Results fom $B^0 \rightarrow \pi^+\pi^-\pi^0$ Dalitz analysis.

The  $B^0 \rightarrow \rho^\pm\pi^\mp$  decay has no final  $CP$  eigenstate like  $\pi^+\pi^-$  or  $\rho^+\rho^-$ . An isospin analysis would not constrain sufficiently the many amplitudes of the  $B$  decays to  $\rho^+\pi^-$ ,  $\rho^-\pi^+$ ,  $\rho^0\pi^0$ ,  $\rho^+\pi^0$ ,  $\rho^0\pi^+$  and their charge conjugates. A better approach [23] is based on the time-dependent analysis of the  $B^0 \rightarrow \pi^+\pi^-\pi^0$  decay over the Dalitz plot, illustrated in Figure 7, using the isospin symmetry as an additional constraint. As this  $B \rightarrow 3\pi$  decay is dominated by  $\rho\pi$  resonances, its amplitude is a function of well-known kinematic functions of the Dalitz variables and of the  $B^0 \rightarrow \rho\pi$  amplitudes, themselves functions of  $\alpha$  and tree and penguin contributions,  $A(B^0 \rightarrow \rho^\kappa\pi^{-\kappa}) = T^\kappa e^{-i\alpha} + P^\kappa$  with  $\kappa=(0, +, -)$ . Only the sign of the weak phase

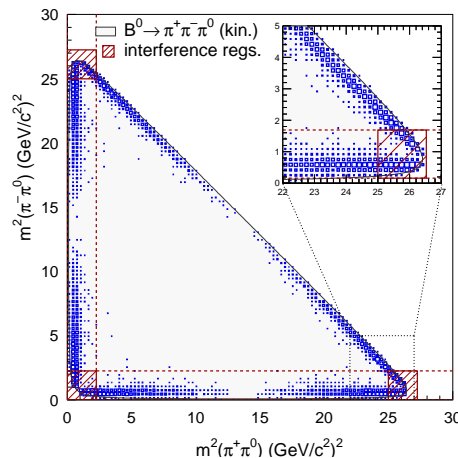


Figure 7: Dalitz plot for Monte Carlo generated  $B^0 \rightarrow \pi^+\pi^-\pi^0$  events. The main overlap regions between the  $\rho$  bands are indicated by the hatched areas.

$\alpha$  is changed when switching to the charge conjugate process. The time-dependent  $CP$  analysis of the  $B^0 \rightarrow \pi^+\pi^-\pi^0$  decay then provides enough constraints to extract  $\alpha$  without discrete ambiguities and the tree and penguin amplitudes.

Technically the analysis is based on a fit of 26 bilinear coefficients. It has been performed by BABAR using  $375 \times 10^6 B\bar{B}$  pairs [24] and Belle using  $449 \times 10^6 B\bar{B}$  pairs [25] corresponding to  $2067 \pm 68$  and  $971 \pm 42$  signal events respectively. The resulting constraint on  $\alpha$  is illustrated in Figure 8. Combining the results of the two experiments is not just an average in  $\alpha$  but a combination in the 26 experimentally measured coefficients, which are correlated among each other. The Dalitz analysis of the  $B \rightarrow \rho\pi$  mode gives a combined value of  $\alpha$  of  $(120_{-8}^{+11})^\circ$ .

#### 5. Study of $B \rightarrow a_1\pi$ decays

The  $B \rightarrow a_1\pi$  modes also allow the measurement of  $\alpha$ . The  $B^0 \rightarrow a_1^\pm\pi^\mp$  channel has a high branching fraction,  $(33 \pm 4 \pm 3)10^{-6}$  as measured by BABAR using  $218 \times 10^6 B\bar{B}$  pairs [26] and  $(30 \pm 3 \pm 5)10^{-6}$  as measured by Belle using  $535 \times 10^6 B\bar{B}$  pairs [27]. The two results are in good agreement and give a world average of  $(32 \pm 4)10^{-6}$ .

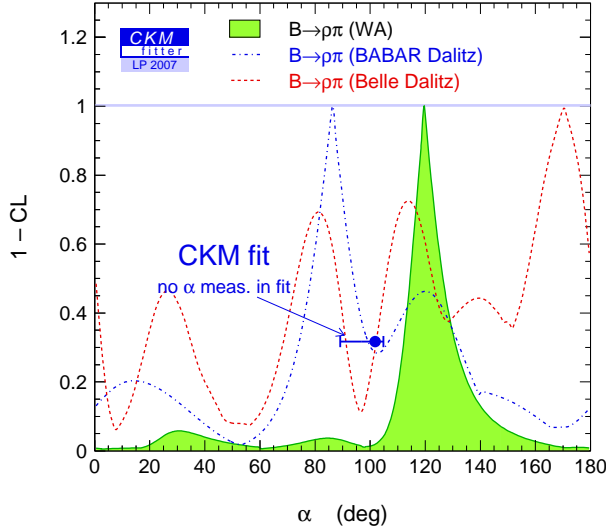


Figure 8: Constraint on  $\alpha$  from the Dalitz analysis in the  $B \rightarrow \rho\pi$  modes. The dot-dashed (dashed) curve uses BABAR (Belle) measurements only, while the hatched region gives the combined constraint.

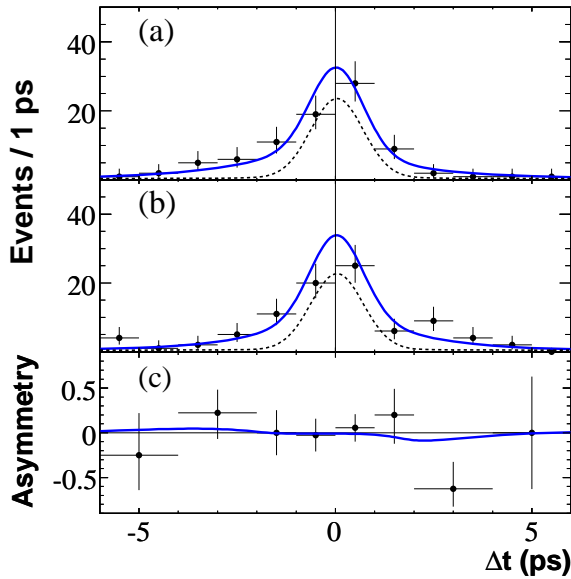


Figure 9: Projections onto  $\Delta t$  of the data (points) for (a)  $B^0$  and (b)  $\bar{B}^0$  tags, showing the fit function (solid line) and the background function (dotted line), and (c) the asymmetry between  $B^0$  and  $\bar{B}^0$  tags.

The  $B^0 \rightarrow a_1^\pm \pi^\mp$  mode, like  $B^0 \rightarrow \rho^\pm \pi^\mp$ , is not a  $CP$  eigenstate. Using a quasi-two body approach, BABAR has performed a time-dependent analysis of this mode based on  $384 \times 10^6 B\bar{B}$  pairs [28]. It is illustrated in Figure 9 by the projection plots onto  $\Delta t$  for  $B^0$  and  $\bar{B}^0$  tags, and the asymmetry between  $B^0$  and  $\bar{B}^0$  tags. From  $608 \pm 52$  signal events, it allows to

measure  $\alpha_{\text{eff}}^{a_1\pi} = (79 \pm 7)^\circ$ .

To constrain  $\alpha - \alpha_{\text{eff}}$  and extract  $\alpha$ , flavor SU(3) symmetry can be used [29]. In addition to  $B \rightarrow a_1\pi$ , the related modes  $B \rightarrow K_1\pi$  and  $B \rightarrow a_1K$  have to be measured. Using  $383 \times 10^6 B\bar{B}$  pairs, BABAR has studied the  $B \rightarrow a_1K$  modes [30] and has measured the branching fractions  $\mathcal{B}(B^0 \rightarrow a_1^- K^+) = (16.3 \pm 2.9 \pm 2.3)10^{-6}$  and  $\mathcal{B}(B^+ \rightarrow a_1^+ K^0) = (34.9 \pm 5.0 \pm 4.4)10^{-6}$ . The  $B \rightarrow K_1\pi$  modes, where  $K_1$  is a mixture of  $K_1(1270)$  and  $K_1(1400)$ , are being searched for. With this last piece of information, a new constraint on  $\alpha$  from the  $B \rightarrow a_1\pi$  modes will be set.

## 6. Summary

Figure 10 summarizes the constraints on  $\alpha$  obtained by BABAR and Belle, from the isospin analysis in the  $B \rightarrow \pi\pi$  and  $B \rightarrow \rho\rho$  modes and the Dalitz analysis in the  $B \rightarrow \rho\pi$  modes. The contribution from the  $B \rightarrow \pi\pi$  modes is limited by the large penguin pollution. The  $B \rightarrow \rho\rho$  mode, slightly improved by the time-dependent  $CP$  analysis of the  $B^0 \rightarrow \rho^0\rho^0$  channel, gives the best single measurement, but has mirror solutions that are disfavored thanks to the Dalitz  $B \rightarrow \rho\pi$  analysis results. The expected measurement of  $\alpha$  in the  $B \rightarrow a_1\pi$  modes will bring additional information.

All the current results yield a combined value of  $\alpha = (87.5_{-5.3}^{+6.2})^\circ$ . This direct measurement of  $\alpha$  is in good agreement with the indirect measurement  $(102_{-13}^{+3})^\circ$  from the global CKM fit.

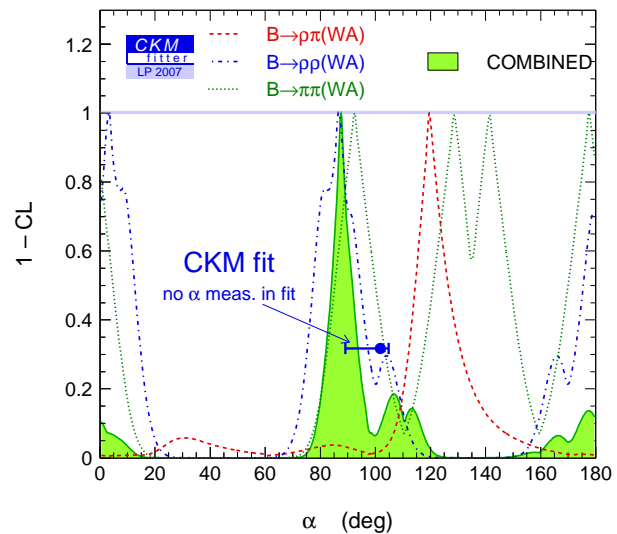


Figure 10: Combined constraint on  $\alpha$ . The individual constraints from the  $B \rightarrow \pi\pi$ ,  $B \rightarrow \rho\rho$ , and  $B \rightarrow \rho\pi$  modes are shown by the dotted, dot-dashed, and dashed curves respectively, while the hatched region gives the combined constraint.

## References

- [1] N. Cabibbo, Phys. Rev. Lett. 10, 531 (1963); M. Kobayashi and T. Maskawa, Prog. Theor. Phys. 49, 652 (1973).
- [2] M. Gronau and D. London, Phys. Rev. Lett. 65, 3381 (1990).
- [3] BABAR Collaboration, B. Aubert *et al.*, Nucl. Inst. and Meth. A 479, 1 (2002); Belle Collaboration, A. Abashian *et al.*, Nucl. Inst. and Meth. A 479, 117 (2002).
- [4] Belle Collaboration, H. Ishino *et al.*, Phys. Rev. Lett. 98, 211801 (2007).
- [5] BABAR Collaboration, B. Aubert *et al.*, Phys. Rev. Lett. 99, 021603 (2007).
- [6] BABAR Collaboration, B. Aubert *et al.*, Phys. Rev. D 75, 012008 (2007).
- [7] BABAR Collaboration, B. Aubert *et al.*, Phys. Rev. D 76, 091102 (2007).
- [8] Belle Collaboration, S.-W. Lin *et al.*, Phys. Rev. Lett. 99, 121601 (2007).
- [9] Belle Collaboration, K. Abe *et al.*, hep-ex/0610065 (2006).
- [10] Belle Collaboration, S.-W. Lin *et al.*, Nature 452, 332 (2008).
- [11] Heavy Flavor Averaging Group (HFAG), <http://www.slac.stanford.edu/xorg/hfag>.
- [12] CKMfitter group, Eur. Phys. J. C41, 1 (2005), updated at <http://ckmfitter.in2p3.fr>.
- [13] Belle Collaboration, A. Somov *et al.*, Phys. Rev. D 76, 011104 (2007).
- [14] BABAR Collaboration, B. Aubert *et al.*, Phys. Rev. D 76, 052007 (2007).
- [15] Belle Collaboration, A. Somov *et al.*, Phys. Rev. Lett. 96, 171801 (2006).
- [16] Belle Collaboration, J. Zhang *et al.*, Phys. Rev. Lett. 91, 221801 (2003).
- [17] C.-C. Chiang for Belle Collaboration, presentation at La Thuile 08 (2008).
- [18] BABAR Collaboration, B. Aubert *et al.*, Phys. Rev. Lett. 97, 261801 (2006).
- [19] BABAR Collaboration, B. Aubert *et al.*, arXiv:0708.1630 (2008).
- [20] M. Beneke *et al.*, Phys. Lett. B 638, 68 (2006).
- [21] Belle Collaboration, J. Zhang *et al.*, Phys. Rev. Lett. 95, 141801 (2005).
- [22] BABAR Collaboration, B. Aubert *et al.*, Phys. Rev. Lett. 97, 201801 (2007).
- [23] A. Snyder and H. Quinn, Phys. Rev. D 48, 2139 (1993).
- [24] BABAR Collaboration, B. Aubert *et al.*, Phys. Rev. D 76, 012004 (2007).
- [25] Belle Collaboration, A. Kusaka *et al.*, Phys. Rev. D 77, 072001 (2008).
- [26] BABAR Collaboration, B. Aubert *et al.*, Phys. Rev. Lett. 97, 051802 (2006).
- [27] Belle Collaboration, K. Abe *et al.*, arXiv:0706.5279 (2007).
- [28] BABAR Collaboration, B. Aubert *et al.*, Phys. Rev. Lett. 98, 181803 (2007).
- [29] M. Gronau and J. Zupan, Phys. Rev. D 73, 057502 (2006).
- [30] BABAR Collaboration, B. Aubert *et al.*, Phys. Rev. Lett. 100, 051803 (2008).